applied sciences

MDPI

Article

Enhanced Crystallinity of $SrTiO_3$ Films on a Silicon Carbide Substrate: Structural and Microwave Characterization

Andrei Tumarkin [1,*], Eugene Sapego [1], Alexey Bogdan [1], Artem Karamov [1], Igor Serenkov [2] and Vladimir Sakharov [2]

[1] Department of Physical Electronics and Technology, Saint Petersburg Electrotechnical University "LETI", 197022 Saint Petersburg, Russia; eugenysapego@yandex.ru (E.S.); alexey.bogdan98@gmail.com (A.B.); temkakaramov@gmail.com (A.K.)

[2] Abram Fedorovich Ioffe Institute of Physics and Technology, Russian Academy of Sciences, 194021 Saint Petersburg, Russia

* Correspondence: avtumarkin@yandex.ru; Tel.: +79-523-792-207

Abstract: Thin films of strontium titanate, which reveal high structure quality and tunable properties prospective for microwave applications at room temperature, were grown on a semi-insulating silicon carbide substrate using magnetron sputtering for the first time. The films' growth mechanisms were studied using medium-energy ion scattering, and the films' structures were investigated using X-ray diffraction. The electrical characteristics of planar capacitors based on strontium titanate films were measured at a frequency of 2 GHz using a high-precision resonance technique. It is shown that the tendency to improve the crystalline structure of strontium titanate film with an increase in the substrate temperature is most pronounced for films deposited at elevated working gas pressure under low supersaturation conditions. Planar capacitors formed on the basis of oriented $SrTiO_3$ films on silicon carbide showed tunability n = 36%, with a loss tangent of 0.008–0.009 at a level of slow relaxation of capacitance, which is significantly lower than the data published currently regarding planar tunable ferroelectric elements. This is the first successful attempt to realize a planar $SrTiO_3$ capacitor on a silicon carbide substrate, which exhibits a commutation quality factor more than 2500 at microwaves.

Keywords: strontium titanate; silicon carbide; thin films; nonlinear dielectric properties; microwave applications

Citation: Tumarkin, A.; Sapego, E.; Bogdan, A.; Karamov, A.; Serenkov, I.; Sakharov, V. Enhanced Crystallinity of $SrTiO_3$ Films on a Silicon Carbide Substrate: Structural and Microwave Characterization. *Appl. Sci.* **2024**, *14*, 9672. https://doi.org/10.3390/app14219672

Academic Editor: Andrea Li Bassi

Received: 13 September 2024
Revised: 14 October 2024
Accepted: 18 October 2024
Published: 23 October 2024

1. Introduction

Electrically tunable devices such as varactors, phase shifters, and delay lines are key elements of modern microwave communication systems. Today, the main materials on the basis of which these devices are implemented are semiconductors, ferrites, and ferroelectrics (FE). All of them have their advantages and disadvantages determined by their physical nature; therefore, the search for the "optimal for microwave applications" material is still an urgent task.

Following is a list of the main desirable characteristics of an "ideal" electrically tunable microwave element: high tunability, low losses, thermal stability of properties, high operating power, and fast response. It is easy to see that a device with such a set of characteristics is not implemented currently. Thus, semiconductor elements operate at low power and significantly lose Q-factor at frequencies above 10 GHz; ferrite elements are characterized by high-energy consumption and dimensions and low speed; the properties of FE devices depend on temperature [1].

It should be noted that FE materials exhibit properties that make them attractive for use in electrically tunable microwave devices, namely a strong dependence on the permittivity on the external electric field [2], relatively low dielectric losses at microwaves [3], the ability

to operate at a high power level [4–7], and fast responses [8]. The above-mentioned properties of FE materials are most effectively realized in film structures on dielectric substrates due to the possibility of forming oriented layers with low microwave losses, the possibility of reaching a high intensity in the control electric field in the film, and the perspective of integration into microwave microelectronic devices [4,8]. Today, laboratory prototypes of electrically tunable capacitors, phase shifters, delay lines, and other microwave elements based on ferroelectric films have been implemented [9–14].

The most studied FE material for microwave applications today is a solid solution of barium and strontium titanates, $Ba_xSr_{1-x}TiO_3$ (BST), the nonlinear properties of which vary widely with changes in the component composition [15,16]. Compositions with a barium content of 50–60%, for which the temperature of the phase transition from ferroelectric to paraelectric state is close to room temperature, exhibit pronounced nonlinear properties, with a low Q–factor and high temperature dependence of the properties [17]. The best combination of tunability and losses, determined by the commutation quality factor [18], is demonstrated by solid solutions with 30% Ba content [15]. A further decrease in the concentration of barium in the solid solution significantly improves the quality factor and reduces the nonlinearity of the material. Pure $SrTiO_3$ (STO) has the lowest microwave loss in this series of solid solutions [19].

Single-crystal strontium titanate is a centrosymmetric paraelectric material with a cubic perovskite structure (a = 3.905 Å), which does not transform into a ferroelectric state when the temperature decreases down to 0 K. The dielectric permittivity ε of the STO crystal increases from 300 at room temperature to 24,000 at 4 K [20]. Strontium titanate is a bright representative of functional oxides. The electrical, optical, thermoelectric, and superconducting properties of $SrTiO_3$ can be used in various electronic devices [21–25]. Strontium titanate films are of interest for strain engineering [26–28], in the development of infrared radiation sensors [29], and for photocatalytic, biosensor [30], and energy-storage [31] applications. Based on strontium titanate films, the epitaxial heterostructures of a "dielectric-semiconductor" [32,33], and multilayer structures for use in photodetectors, memory [34] and other devices [35,36] can be realized. The electrical properties of strontium titanate, which make it a promising material for tunable microwave elements, are considered in [37]. Summarizing the conclusions of this work, it should be noted that in addition to high ε and low dielectric losses, tunable elements based on STO films exhibit a nonlinear dependence of the permittivity on the electric field, high response speed, and a weak temperature dependence of the properties at room temperature.

A separate challenge is the development of high-power tunable FE microwave elements. One of the most important characteristics of these elements is their ability to operate at a high level of microwave power without distortion of the capacitance and quality factors. These distortions occur under the influence of electrical and thermal effects. Electrical distortions caused by the nonlinearity of the FE material are inevitable in ferroelectric microwave devices. They are successfully used in nonlinear devices or can be minimized in tunable filters and phase shifters [38,39]. The scale of thermal distortions caused by microwave power dissipation is determined by the thermal conductivity of the dielectric substrate [40]. Today, high-quality strontium titanate films are grown on various mono- and polycrystalline substrates such as MgO [41], $LaAlO_3$ [19], sapphire [42], alumina [37], and $DyScO_3$ [26–28]. Magnesium and aluminum oxides have the best heat-conducting characteristics of the above materials [43,44]. The thermal conductivity coefficients of MgO and Al_2O_3 are between the order of 60 and 40 $W \cdot m^{-1} \cdot K^{-1}$, respectively, which does not allow them to avoid overheating ferroelectric microwave elements on these substrates [11,38,39].

Semi-insulating silicon carbide (SiC) appears to be a promising substrate material that can significantly improve the power characteristics of FE elements. The material has a thermal conductivity coefficient of 500 $W \cdot m^{-1} \cdot K^{-1}$, high strength, low dielectric losses [45,46], and proven production technology. Thus, tunable high Q-factor elements based on strontium titanate films on silicon carbide substrates are potentially promising for high-power microwave applications.

Today, a number of works devoted to the growth of FE films on silicon carbide have been published [47–50]. All of these works consider elements based on BST films, the highest quality factor of which does not exceed 50 at microwaves. Publications devoted to strontium titanate films on silicon carbide are absent in the modern literature. In connection with the above, the objective of this work is to synthesize strontium titanate films of high structural quality on semi-insulating silicon carbide substrates for their further use in powerful high-Q-factor microwave tunable devices. For this purpose, we investigated the relationships between the technological conditions of film deposition, the mechanisms of their nucleation and growth on SiC substrates, and their structural and electrical characteristics. Studies on the growth mechanisms of strontium titanate films were carried out on island structures sensitive to changes in technological parameters. The relationship between the structural characteristics and key technological factors, namely substrate temperature and working gas pressure, was studied using X-ray structural analysis. The electrical characteristics of the films with the best crystal structure were studied using resonance techniques using planar capacitors at microwaves.

2. Experimental

2.1. Synthesis of Thin Films

Thin films of strontium titanate were deposited on substrates of semi-insulating silicon carbide using high-frequency magnetron sputtering. SiC substrates of hexagonal polytype 6H with a diameter of 76 mm and lattice parameters a = 0.308 nm, c = 1.512 nm of "epi-ready" quality were manufactured at "Svetlana Electronpribor" St. Petersburg. The dimensions of the substrate for film growth were 10 × 10 mm with a thickness of 0.4 mm. A ceramic target of stoichiometric composition $SrTiO_3$ with a diameter of 76 mm was manufactured using the method of single-stage solid-phase synthesis from a mixture of chemically pure $SrCO_3$ and TiO_2 powders at the St. Petersburg Institute "Ferrite-Domain".

Before the film deposition process, the vacuum chamber was pumped out to a residual pressure of 10^{-3} Pa. The films were synthesized at substrate temperatures T_s in the range of 600–900 °C. A mixture of Ar:O_2 (3:1) was used as the working gas during deposition, the pressure of the working gas P varied in the range of 3–10 Pa. To study the mechanisms of STO film growth on SiC substrates, island films with a thickness of several nanometers were made. These films were deposited for 20–100 s at working gas pressures of between 6 and 10 Pa and at substrate temperatures of between 800 and 900 °C. The deposition time of the solid films varied from 120 to 360 min, depending on the pressure of the working gas, in order to obtain films with thicknesses of 500–800 nm. The process of growing continuous films began at a pressure of 10 Pa; then, if necessary, the pressure was lowered to the required value during the first 30 min of the process.

2.2. Investigation Techniques

The structure of island films formed at the initial stages of growth was studied using the medium-energy ion scattering (MEIS) method. The samples were bombarded with helium ions with an initial energy of 227 keV. The ion energy after interaction with atoms of the film was registered using an electrostatic analyzer. The crystal structure and phase composition of continuous films were controlled using X-ray phase analysis (XRD) on a DRON-6 diffractometer at the Cu Kα1 emission spectral line (λ = 1.54 Å). Measurements were carried out in continuous mode at diffraction angles from 20° to 60° with a scanning speed of 2°/min. Crystal phases were identified using the PDF-2 powder diffractometry database. To calculate the unit cell parameters of STO films investigated, the angular positions of their reflections were used, taking the peak from the substrate as a reference. The surface morphology was investigated using the atomic force microscopy method (AFM) on a scanning probe microscope NTEGRA PRIMA from NT-MDT in semi-contact mode. The scanning resolution was 512 × 512 pixels. Cantilevers of the NSG01 type with an average resonant frequency of 150 kHz and an average radius of curvature of the tip of

6 nm were used. Before the measurements, the device was calibrated using NT-MDT TGS1 test grids.

The electrical properties of STO films were investigated using planar capacitors with a gap width of 6 μm. Copper electrodes were applied on the surface of the STO film using the thermal evaporation technique using an adhesive chromium sublayer, followed by lithography and chemical etching. The capacitance C and quality factor Q = 1/tan δ of the capacitors were measured at a frequency of 2 GHz using a half-wave stripline resonator and an HP 8719C vector analyzer. The resonator design provides an unloaded quality factor of 1000, which ensures the accuracy of capacitance and quality factor measurements of 1 and 5%, respectively. A control voltage of up to 300 V was applied directly to the capacitor plates, providing a field strength E in the capacitor gap of up to 50 V/μm. The tunability of the capacitors was calculated as the ratio of capacitances at zero and maximum applied control voltage $n = (C_{max} - C_{min})/C_{max}$.

3. Results and Discussion

3.1. Initial Stages of STO Film Growth

The structure, phase composition, and electrical properties of multicomponent films depend on the conditions under which the initial stages of layer growth are realized—nucleation and coalescence. The mechanisms of nucleation are determined by the competition of desorption, surface diffusion, and nucleation processes, the intensity of which, in turn, depends on the substrate temperature and the working gas pressure. It is known [51,52] that the formation of highly oriented multicomponent film is realized during the deposition of vapors with low supersaturation. In this case, the free energy of formation of oriented islands is lower than the free energy of formation of unoriented three-dimensional nuclei. Consequently, in order to grow oriented films, at the stage of their nucleation, it is advisable to create conditions that ensure weak supersaturation.

The effect of technological parameters on the growth mechanisms of strontium titanate-like BST films on silicon carbide was studied in [53]. In this work, it was shown that the deposition of FE films on silicon carbide at working gas pressures of about 10 Pa makes it possible to realize low condensation rates determined using supersaturation, while a substrate temperature of 900 °C ensures active diffusion of adatoms before their attachment to the islands. Thus, oriented crystallization processes on the substrate's surface are stimulated, which can lead to the formation of predominantly oriented films. In this regard, in this work, the initial stages of STO film growth on silicon carbide were studied at temperatures of 800–900 °C and pressures of 6–10 Pa.

When studying the mechanisms of nucleation of strontium titanate films on silicon carbide substrates, the analysis of the energy spectra of backscattered ions from STO island films makes it possible to determine the geometric dimensions of the islands, the spread of their heights, and the degree of filling of the substrate with islands [54]. Figure 1 shows the spectra of helium ions after their interaction with island films deposited at different working gas pressures and substrate temperatures. It can be seen from the graph that the spectra of films deposited at pressures of 6 and 10 Pa are similar to each other, which indicates similar mechanisms of film formation in this pressure range. The peaks corresponding to ion scattering on the heavy elements of the film have an asymmetric triangular shape with an overextended low-energy front. A comparison of the model and experimental spectra obtained from films deposited at pressures of between 6 and 10 Pa allows us to conclude that the height of the islands is 3–4 nm and the degree of filling of the substrate with islands is 75% at the same amount of substance on the surface of the substrate. The shape of the spectra indicates an island height spread of about 50%, which corresponds to the film growth mechanism of Volmer–Weber.

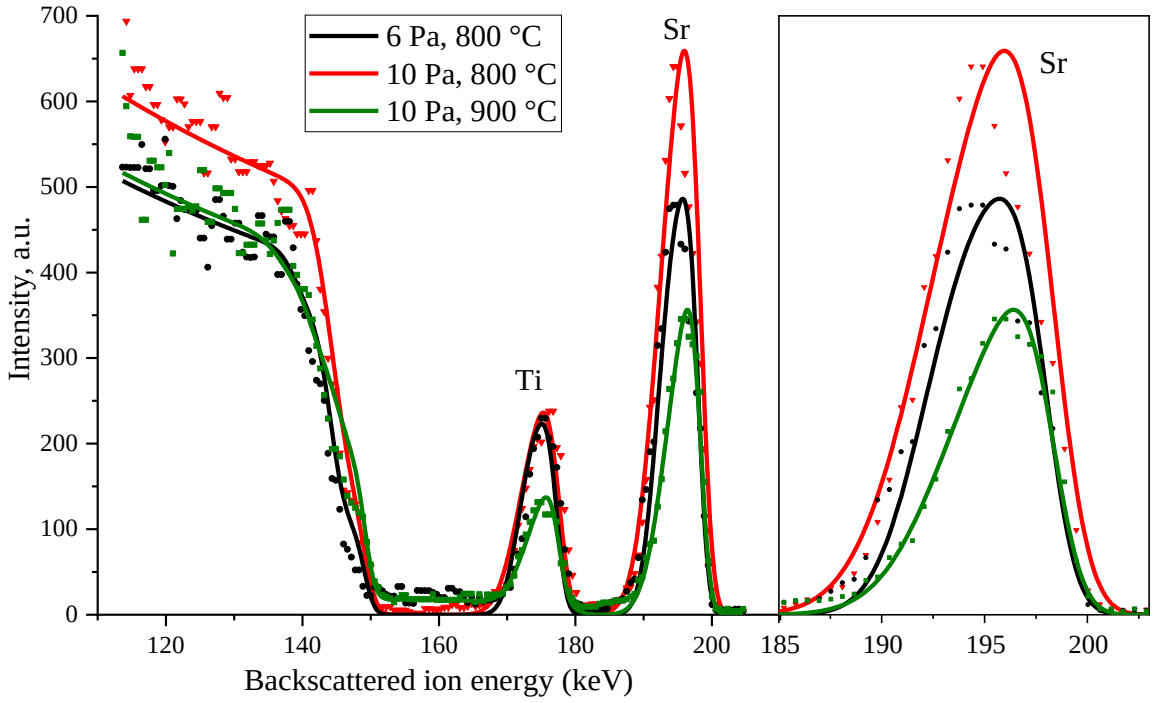

Figure 1. MEIS spectra of STO films obtained at pressures of 6 and 10 Pa and at substrate temperatures of 800–900 °C.

The spectrum of backscattered ions from the film deposited at a temperature of 900 °C demonstrates the most prolonged low-energy front, which indicates a greater dispersion of islands in size. Analysis of the graphs for films deposited at different substrate temperatures allows us to draw conclusions similar to the previous ones, with the difference being that the amount of substance on the substrate heated to 900 °C is two times less than in the case of T_s = 800 °C (the height of the islands is about 3–5 nm, but the degree of coverage decreases from 75 to 50%). It is obvious that at T_s = 900 °C, the intensity of re-evaporation of adatoms from the substrate surface increases.

Figure 2 shows the dependence of the height of the islands and the degree of filling of the substrate with islands on the deposition time of the films. The dynamics of changes in the thickness of the film and the area of the substrate occupied by the islands allow us to conclude that under these conditions, at deposition times from 20 to 50 s, the stage of the formation of islands as a result of the fusion of small nuclei, the so-called primary coalescence, is realized. At this stage, the main mass transfer is carried out by diffusion of the substance over the substrate in the spaces between the islands. After 50 c of deposition, the island formation stage is replaced by a secondary coalescence stage, when the fusion of the islands begins to form a single structure in the form of a grid. At this stage, the degree of coating of the substrate surface with a condensed substance increases sharply due to a change in the shape of the islands to a flatter one. This stage of film growth is characterized by significant mass transfer over the surface of the accreting island grains [52].

The study of the stages of nucleation and coalescence of strontium titanate films on silicon carbide allows us to draw the following conclusions. In the considered ranges of substrate temperatures and working gas pressures, which ensure condensation at low supersaturation, the process of STO phase nucleation on the SiC surface occurs according to the Volmer–Weber island mechanism. The implementation of this growth mechanism in the STO-SiC system is determined by the mismatch between the hexagonal substrate structure and the cubic film one, and their weak interphase bond [50]. At the same time, weak supersaturation provides conditions for the formation of oriented STO islands, which allows us to expect the growth of a highly oriented film in the future.

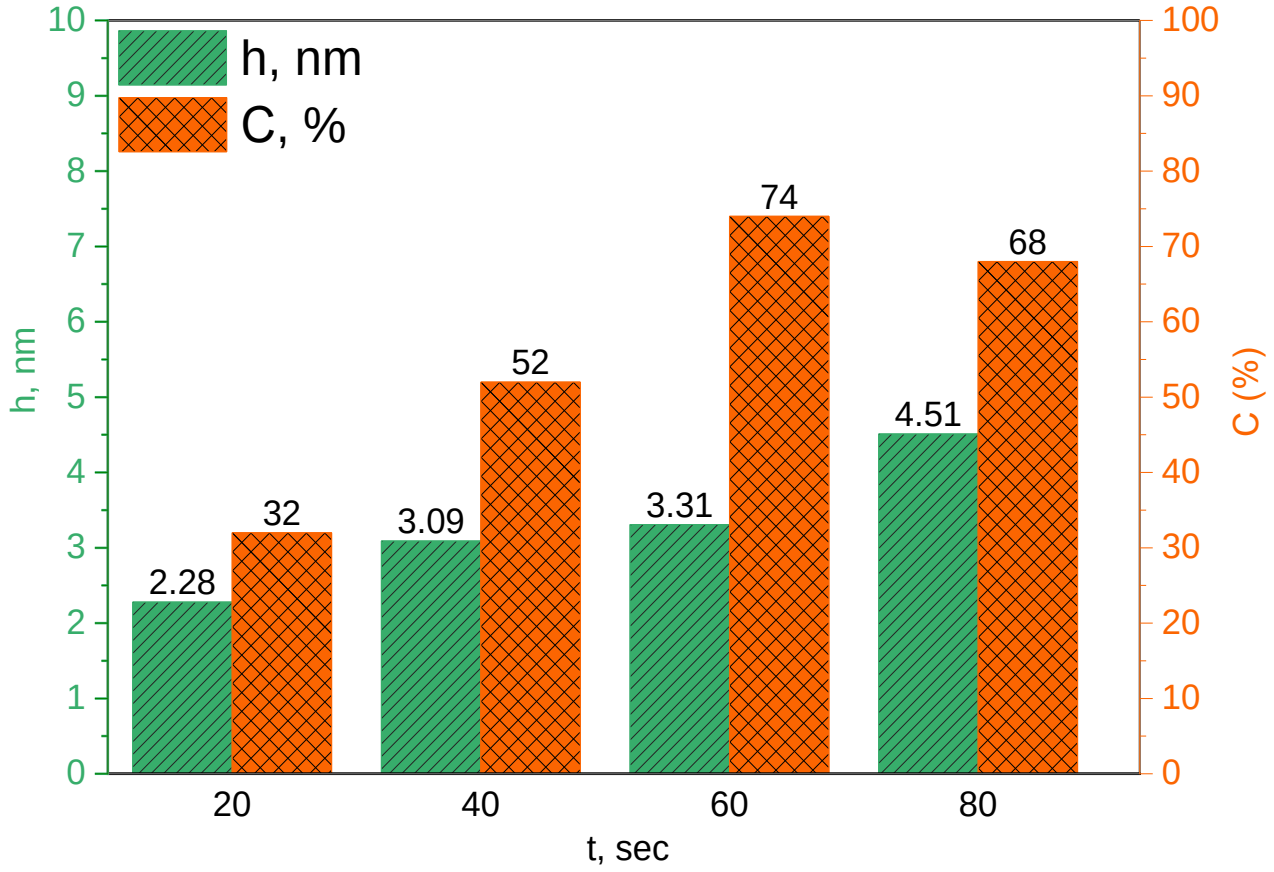

Figure 2. The height of the islands and the degree of coating of the substrate with islands for STO films grown at T_s = 800 °C.

3.2. Structure Characterization of STO Films

Figure 3 shows the diffraction patterns of STO films on silicon carbide deposited at different substrate temperatures and working gas pressures. The positions of reflections for bulk strontium titanate (PDF 35–734) are marked with vertical dotted lines, and the reflections of the substrate are marked with diamonds. The diffraction patterns for all the studied samples confirm the formation of pure strontium titanate with a perovskite structure. The films formed at a low substrate temperature are polycrystalline and strained—the diffraction patterns contain reflections (110) and (200), the position of which differs from the positions of reflections of an unstrained STO crystal. With an increase in the deposition temperature, the intensity of the reflection (200) increases and the angular positions of the peaks shift toward larger angles, which means a decrease in the unit cell parameter from 3.95 to 3.907 Å. These trends are typical for all the considered working gas pressures, and indicate a significant improvement in the crystal structure of STO films and a decrease in internal stresses in the lattice.

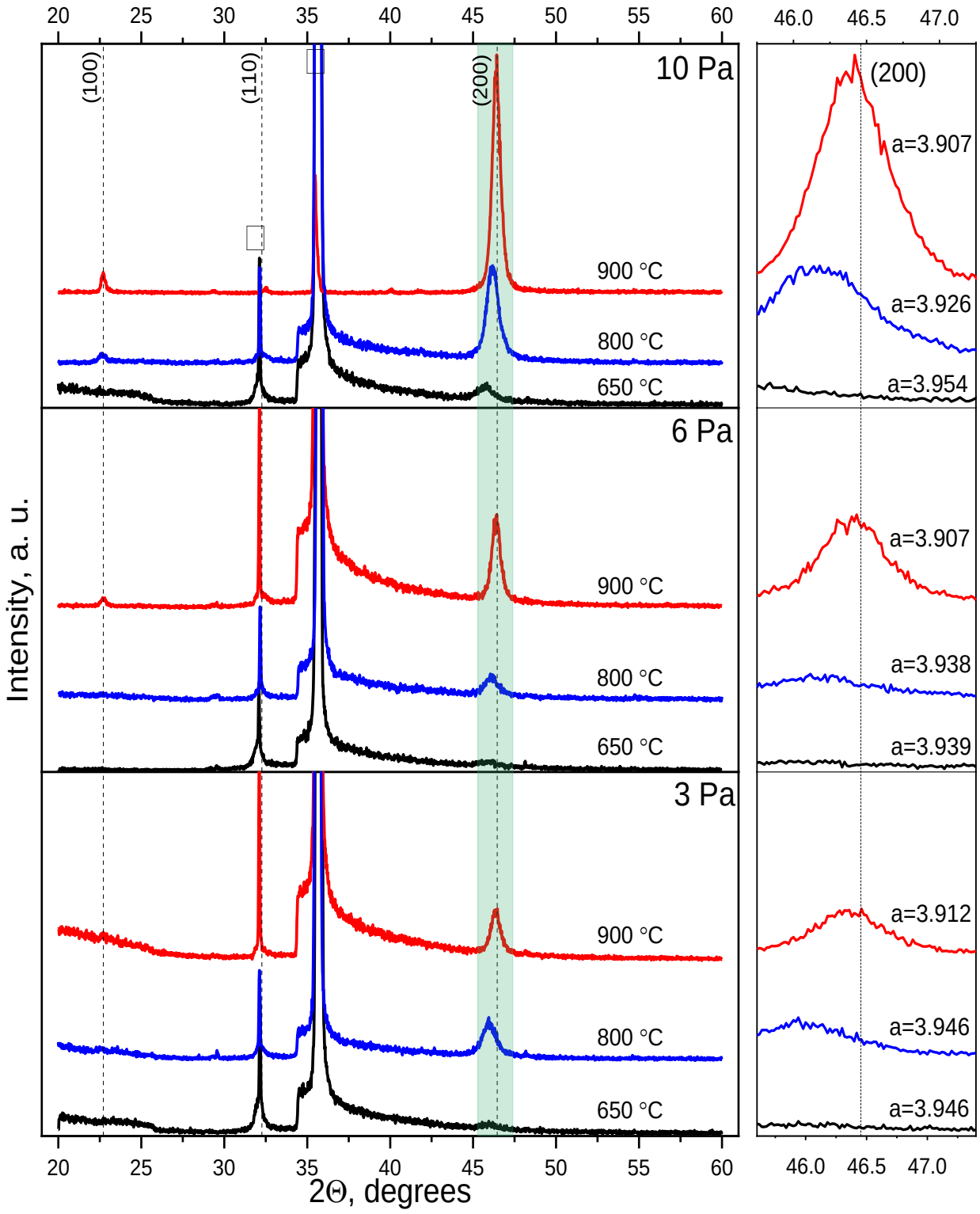

Figure 3. Diffractograms of films obtained at different substrate temperatures and different working gas pressures.

Let us compare the diffraction patterns of STO films deposited at T_s = 900 °C, but at different pressures. The films exhibit a single-phase predominantly oriented structure (h00) at the absence of internal stresses in the lattice. The high temperature of the substrate ensures the active surface diffusion of particles before their incorporation into the STO lattice, which leads to the formation of an unstressed defect-free film. In addition, the

intensity of the (200) reflex of the film deposited at a pressure of 10 Pa is half an order of magnitude higher than the intensity of similar peaks of films formed at low pressures. Thus, the tendency to improve the structure is most pronounced for films deposited at elevated working gas pressure, which confirms the thesis of oriented crystallization at low supersaturation. Figure 4 shows comparative diffractograms of films of various thicknesses deposited under optimal conditions from the structure point of view (T_s = 900 °C, P = 10 Pa). With an increase in the thickness of the STO film, a significant improvement in its crystal structure is observed—the intensity of the (200) reflex increases significantly, and the peak width (FWHM ≅ 0.6°) decreases to values close to those for a single crystal (FWHM ≅ 0.3°). Trends in improving the structural quality of strontium titanate films with an increase in their thickness are noted in [55,56].

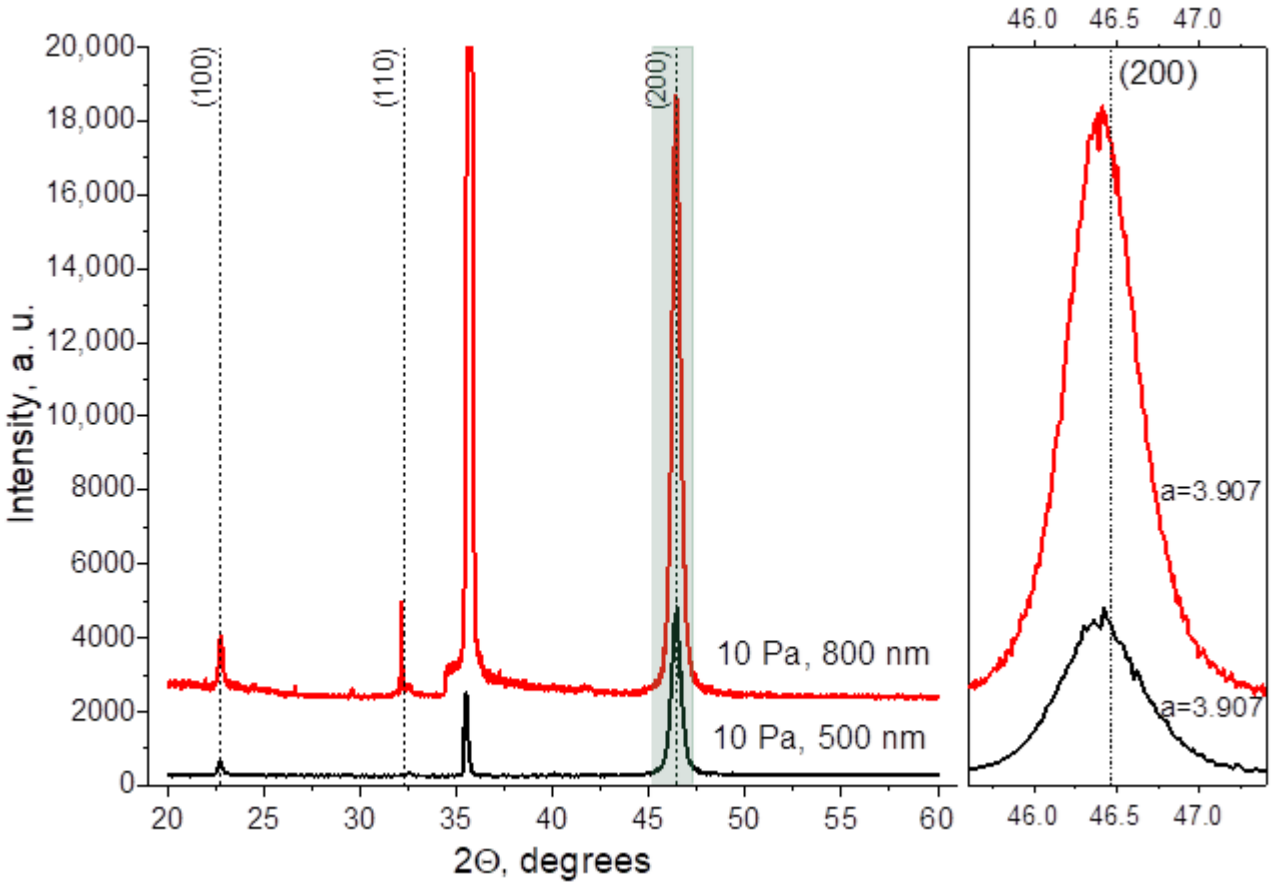

Figure 4. Diffractograms of films of different thicknesses obtained at a pressure of 10 Pa and a substrate temperature of 900 °C.

Figure 5 shows a typical image of the surface of an STO film on silicon carbide obtained using atomic force microscopy. The surface is a homogeneous granular structure without visual defects with grain sizes of about 100–150 nm and a surface roughness of 10–20 nm. The films under study have similar surface morphology, which is determined by the island growth mechanism in the considered technological regimes.

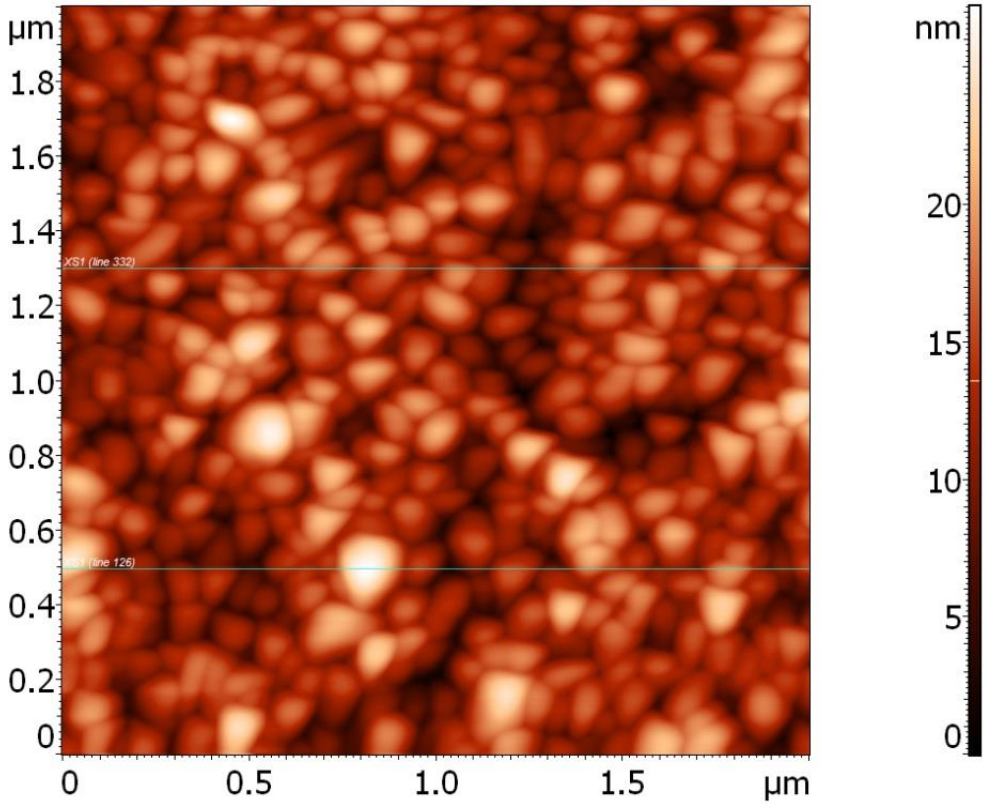

Figure 5. AFM image of a STO film surface on a SiC substrate.

3.3. Electrical Properties of STO Planar Capacitive Structures

The electrical properties of STO films were studied on the samples that demonstrated the best structural characteristics. Figures 6 and 7 show the normalized capacitance, response time parameter, and quality factors of planar capacitors formed on the base of STO films on silicon carbide, depending on the control field strength. For comparison, the figures also show the characteristics of the capacitors based on the STO film deposited at T_s = 650 °C and which had a significantly worse structure. The graphs show that the nonlinearity and microwave losses of the capacitors correlate with the structural quality of the films under study. Capacitors formed on the basis of films deposited at P = 10 Pa and having a minimum number of structural defects and internal stresses exhibit a tunability of 36% at a quality factor of 120–105, while capacitive structures on films deposited at 3 Pa—32.7% at a quality factor of 85–115. Noteworthy are the dynamics of decreasing capacitance with increasing control field strength and the absence of a flat section of the C-V characteristic at a field strength of more than 30 V/µm. This indicates that the tunability of the studied capacitors is far from saturation and that the nonlinearity of the structures can be increased by increasing the level of control action. The best combination of tunability and losses of capacitive elements can be determined based on the commutation quality factor CQF. According to [1], for effective use in microwaves, a capacitive element should demonstrate a CQF of at least 1000. Table 1 shows the comparative electrical characteristics of the studied capacitors—capacitance, quality factor, tunability, and the CQF calculated on their basis. A CQF value of more than 2500 allows us to expect the promising characteristics of controlled microwave elements based on STO/SiC films.

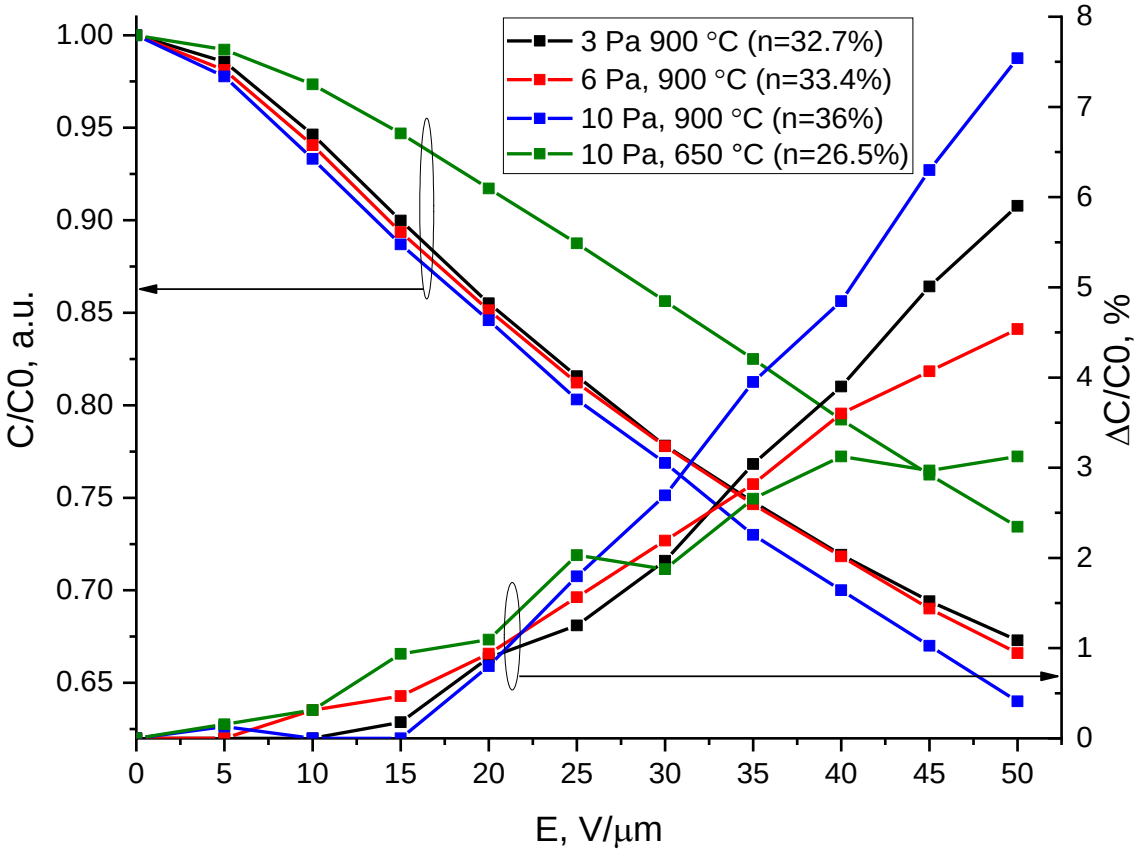

Figure 6. Normalized capacitance and response time parameters of capacitors obtained at different working gas pressures.

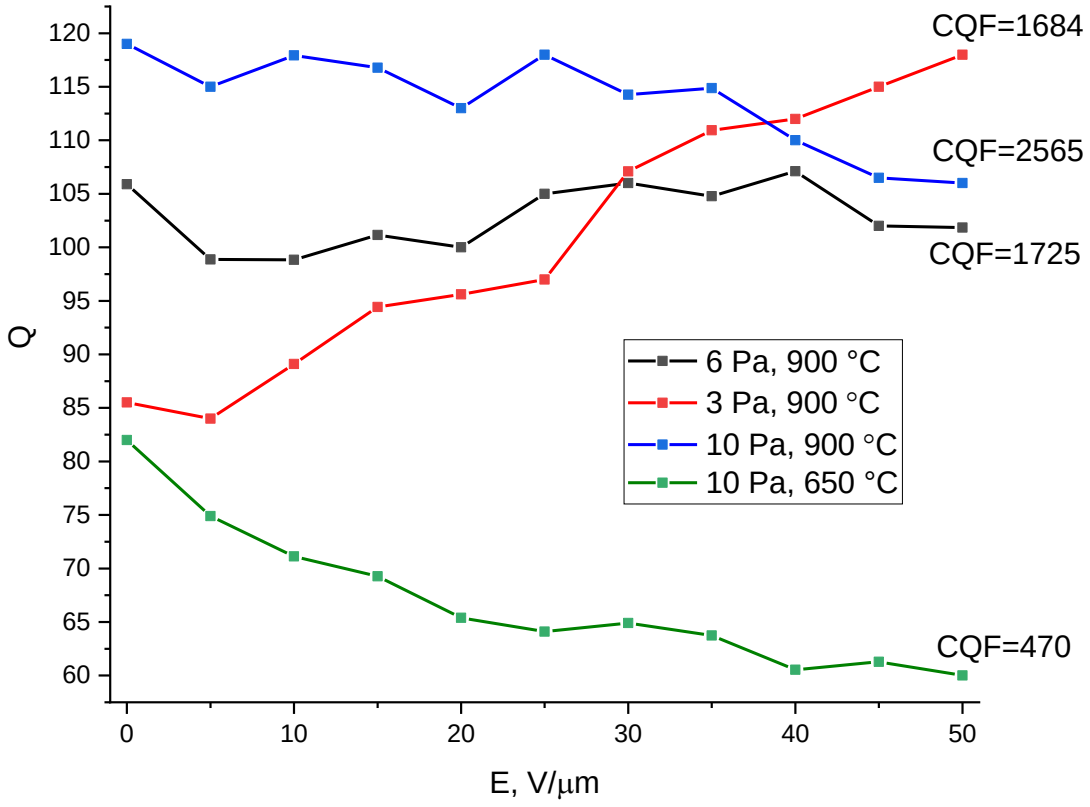

Figure 7. Quality factor of capacitors obtained at different working gas pressures.

Table 1. Comparative electrical characteristics of capacitors based on STO films on silicon carbide.

T_s, °C;	P, Па	Tunability, %	tgδ (U0)	tgδ (U_{max})	CQF (2 GHz)
900	3	32.7	0.009	0.01	1725
	6	33.4	0.012	0.0085	1684
	10	36	0.008	0.009	2565
650	10	26.5	0.012	0.016	470

One of the most important parameters of microwave device operation is its response speed, i.e., the reaction rate of the permittivity to the application and removal of the control action. For tunable elements based on FE films in the paraelectric state (in the absence of spontaneous polarization), a decrease in ε under the action of the control field occurs in times of the order of 10^{-9} s [57], which is due to the fundamental properties of ferroelectrics. However, when the control voltage is removed, a slow relaxation of the capacitance to the initial value can be observed in FE capacitive elements. This relaxation is associated with the formation and redistribution of space charge, which significantly reduces the response speed of FE devices and can be an obstacle to pulse control of the FE element. The main reason for the formation of space charge in a film in the paraelectric phase is considered to be the injection of charge carriers from the electrodes and their capture by defects in the volume of the film [57]. Figure 6 shows the response time parameter ΔC/C0 of the studied STO capacitors, which reflects the capacitance 100 ms after the control voltage is removed. It is evident that the tunability of 36% is accompanied by the non-return of the capacitance by a value not exceeding 7.5%, which is a promising result for use in devices with fast switching. Regarding the response time characteristics of strontium titanate, two important points should be noted. Firstly, until now, the response time of capacitors based on STO films has been estimated only at cryogenic temperatures and only for elements on Al_2O_3 and $GaNdO_3$ substrates [58,59]. Thus, this paper presents, for the first time, data on the slow relaxation of the capacitance of controlled elements based on STO films on silicon carbide at room temperature. Secondly, the scale of slow relaxation of the capacitance of FE elements depends significantly on the capacitor design. For planar BST structures at room temperature, it is estimated at 12% at a control field strength of 10 V/μm [57]. The results obtained in this work ΔC/C0 < 7.5% at a field strength of 50 V/μm are explained by the high structural quality of STO films, and are a significant improvement in the level of non-return of the capacitance of FE planar structures.

4. Conclusions

Predominantly oriented, unstrained strontium titanate films of high structural quality were grown for the first time on semi-insulating silicon carbide substrates using magnetron sputtering. Investigations of the initial stages of STO film growth on silicon carbide showed that in the considered ranges of substrate temperatures and working gas pressures, the nucleation of the STO phase on the SiC surface occurs via the Volmer–Weber island mechanism, caused by the structural mismatch between the substrate and the film and their weak interphase bond. According to the X-ray diffraction analysis, with an increase in the deposition temperature, there is a significant improvement in the crystal structure and minimization of internal stresses in the STO film lattice. The tendency to improve the structure is most pronounced for films deposited at elevated working gas pressure under low supersaturation conditions. Planar capacitors formed on the basis of oriented STO films on silicon carbide showed tunability n = 36% at the level of microwave losses and response time parameters, which are significantly better than the data published today for planar BST elements. A CQF value of more than 2500 allows us to expect promising characteristics in high-power tunable microwave elements based on STO films on SiC. The results obtained show that tunable capacitors and phase shifters for high-power microwave systems can be implemented based on $SrTiO_3$/SiC planar structures. The development of

designs and implementation of phased antenna arrays based on high-Q phase shifters in the frequency range of 1–15 GHz seems promising. To achieve this goal, the next step of our research is planned to be the search for technological ways to increase the tunability of STO capacitors, studying them at elevated levels of microwave power, with the purpose of their further application as lumped tunable elements in microwave phase shifters.

Author Contributions: Conceptualization A.T.; Methodology, A.T.; Software, I.S. and V.S.; Validation A.T. and A.B.; Investigation A.T., E.S., A.B., A.K. and V.S.; Resources, A.T., I.S. and V.S.; Data Curation, A.T., I.S. and V.S.; Writing—Original Draft Preparation, A.T.; Writing—Review and Editing, A.T. and A.B.; Visualization, E.S., A.B. and A.K.; Supervision, A.T.; Project Administration, E.S.; Funding Acquisition, A.T. All authors have read and agreed to the published version of the manuscript.

Funding: This research was funded by the grant of The Ministry of Education and Science of Russian Federation (project Goszadanie № 075-01438-22-07 FSEE-2022-0015). Igor Serenkov and Vladimir Sakharov worked independently of grant support.

Institutional Review Board Statement: Not applicable.

Informed Consent Statement: Not applicable.

Data Availability Statement: The original contributions presented in the study are included in the article, further inquiries can be directed to the corresponding author.

Conflicts of Interest: The authors declare no conflict of interest.

References

1. Vendik, O.G. Ferroelectrics Find Their "Niche" among Microwave Control Devices. *Phys. Solid. State* **2009**, *51*, 1529–1534. [CrossRef]
2. Carlson, C.M.; Rivkin, T.V.; Parilla, P.A.; Perkins, J.D.; Ginley, D.S.; Kozyrev, A.B.; Oshadchy, V.N.; Pavlov, A.S. Large Dielectric Constant (ε/ε>;6000) $Ba_{0.4}Sr_{0.6}TiO_3$ Thin Films for High-Performance Microwave Phase Shifters. *Appl. Phys. Lett.* **2000**, *76*, 1920–1922. [CrossRef]
3. Li, S.; Wang, Y.; Yang, M.; Miao, J.; Lin, K.; Li, Q.; Chen, X.; Deng, J.; Xing, X. Ferroelectric Thin Films: Performance Modulation and Application. *Mater. Adv.* **2022**, *3*, 5735–5752. [CrossRef]
4. Martin, L.W.; Rappe, A.M. Thin-Film Ferroelectric Materials and Their Applications. *Nat. Rev. Mater.* **2016**, *2*, 16087. [CrossRef]
5. Xu, Y. *Ferroelectric Materials and Their Applications*; Elsevier Science: Amsterdam, The Netherlands, 2013; ISBN 978-1-4832-9095-9.
6. Tagantsev, A.K.; Sherman, V.O.; Astafiev, K.F.; Venkatesh, J.; Setter, N. Ferroelectric Materials for Microwave Tunable Applications. *J. Electroceramics* **2003**, *11*, 5–66. [CrossRef]
7. Vendik, O.G.; Zubko, S.P.; Nikol'skii, M.A. Modeling and Calculation of the Capacitance of a Planar Capacitor Containing a Ferroelectric Thin Film. *Tech. Phys.* **1999**, *44*, 349–355. [CrossRef]
8. Fernandez, A.; Acharya, M.; Lee, H.; Schimpf, J.; Jiang, Y.; Lou, D.; Tian, Z.; Martin, L.W. Thin-Film Ferroelectrics. *Adv. Mater.* **2022**, *34*, 2108841. [CrossRef]
9. Borderon, C.; Ginestar, S.; Gundel, H.W.; Haskou, A.; Nadaud, K.; Renoud, R.; Sharaiha, A. Design and Development of a Tunable Ferroelectric Microwave Surface Mounted Device. *IEEE Trans. Ultrason. Ferroelect. Freq. Control* **2020**, *67*, 1733–1737. [CrossRef]
10. Abdulazhanov, S.; Le, Q.H.; Huynh, D.K.; Wang, D.; Lehninger, D.; Kämpfe, T.; Gerlach, G. THz Thin Film Varactor Based on Integrated Ferroelectric $HfZrO_2$. *ACS Appl. Electron. Mater.* **2023**, *5*, 189–195. [CrossRef]
11. Tumarkin, A.; Gagarin, A.; Zlygostov, M.; Sapego, E.; Altynnikov, A. Heterostructures "Ferroelectric Film/Silicon Carbide" for High Power Microwave Applications. *Coatings* **2020**, *10*, 247. [CrossRef]
12. Zeinar, L.; Salg, P.; Walk, D.; Petzold, S.; Arzumanov, A.; Jakoby, R.; Maune, H.; Alff, L.; Komissinskiy, P. Matching Conflicting Oxidation Conditions and Strain Accommodation in Perovskite Epitaxial Thin-Film Ferroelectric Varactors. *J. Appl. Phys.* **2020**, *128*, 214104. [CrossRef]
13. Bouca, P.; Pinho, R.; Wlodarkiewicz, A.; Tkach, A.; Matos, J.N.; Vilarinho, P.M.; De Carvalho, N.B. RF Phase Shifters Design Based on Barium Strontium Titanate Thick and Thin Films. In Proceedings of the 2022 IEEE MTT-S International Conference on Microwave Acoustics and Mechanics (IC-MAM), Munich, Germany, 18–20 July 2022; IEEE: Munich, Germany, 2022; pp. 1–4. [CrossRef]
14. Dey, S.; Koul, S.K.; Poddar, A.K.; Rohde, U. RF MEMS Switches, Switching Networks and Phase Shifters for Microwave to Millimeter Wave Applications. *ISSS J. Micro Smart Syst.* **2020**, *9*, 33–47. [CrossRef]
15. Razumov, S.V.; Tumarkin, A.V.; Gaidukov, M.M.; Gagarin, A.G.; Kozyrev, A.B.; Vendik, O.G.; Ivanov, A.V.; Buslov, O.U.; Keys, V.N.; Sengupta, L.C.; et al. Characterization of Quality of $Ba_xSr_{1-x}TiO_3$ Thin Film by the Commutation Quality Factor Measured at Microwaves. *Appl. Phys. Lett.* **2002**, *81*, 1675–1677. [CrossRef]
16. Zhu, X.; Zhu, J.; Zhou, S.; Liu, Z.; Ming, N.; Lu, S.; Chan, H.L.-W.; Choy, C.-L. Recent Progress of (Ba,Sr)TiO_3 Thin Films for Tunable Microwave Devices. *J. Electron. Mater.* **2003**, *32*, 1125–1134. [CrossRef]

17. Kozyrev, A.; Keis, V.; Buslov, O.; Ivanov, A.; Soldatenkov, O.; Loginov, V.; Taricin, A.; Graul, J. Microwave Properties of Ferroelectric Film Planar Varactors. *Integr. Ferroelectr.* **2001**, *34*, 271–278. [CrossRef]
18. Vendik, I.B.; Vendik, O.G.; Kollberg, E.L. Criterion for a Switching Device as a Basis of Microwave Switchable and Tunable Components. In Proceedings of the 1999 29th European Microwave Conference, Munich, Germany, 5–7 October 1999; IEEE: Munich, Germany, 1999; pp. 187–190. [CrossRef]
19. Panomsuwan, G.; Saito, N. Thickness-Dependent Strain Evolution of Epitaxial $SrTiO_3$ Thin Films Grown by Ion Beam Sputter Deposition. *Cryst. Res. Technol.* **2018**, *53*, 1700211. [CrossRef]
20. Müller, K.A.; Burkard, H. $SrTiO_3$: An Intrinsic Quantum Paraelectric below 4 K. *Phys. Rev. B* **1979**, *19*, 3593–3602. [CrossRef]
21. Mudhaffar, A.; Al-Jawhari, H. Impact of Deep Ultraviolet-Ozone Photoactivation on Dielectric Properties of Amorphous $SrTiO_3$ Thin Films. *KEM* **2022**, *907*, 17–23. [CrossRef]
22. Gueckelhorn, D.; Kersch, A.; Ruediger, A. Strain-Induced Enhancement of Surface Self-Diffusion on Strontium Titanate (001) Surfaces. *J. Phys. Condens. Matter* **2024**, *36*, 415002. [CrossRef]
23. Janicki, T.D.; Liu, R.; Im, S.; Wan, Z.; Butun, S.; Lu, S.; Basit, N.; Voyles, P.M.; Evans, P.G.; Schmidt, J.R. Mechanisms of Three-Dimensional Solid-Phase Epitaxial Crystallization of Strontium Titanate. *Cryst. Growth Des.* **2024**, *24*, 7406–7414. [CrossRef]
24. Hameed, S.; Pelc, D.; Anderson, Z.W.; Klein, A.; Spieker, R.J.; Yue, L.; Das, B.; Ramberger, J.; Lukas, M.; Liu, Y.; et al. Enhanced Superconductivity and Ferroelectric Quantum Criticality in Plastically Deformed Strontium Titanate. *Nat. Mater.* **2022**, *21*, 54–61. [CrossRef] [PubMed]
25. Wang, S.; Gao, H.; Yu, X.; Tang, S.; Wang, Y.; Fang, L.; Zhao, X.; Li, J.; Yang, L.; Dang, W. Nanostructured $SrTiO_3$ with Different Morphologies Achieved by Mineral Acid-Assisted Hydrothermal Method with Enhanced Optical, Electrochemical, and Photocatalytic Performances. *J. Mater. Sci. Mater. Electron.* **2020**, *31*, 17736–17754. [CrossRef]
26. Chang, W.; Kirchoefer, S.W.; Bellotti, J.A.; Qadri, S.B.; Pond, J.M.; Haeni, J.H.; Schlom, D.G. In-Plane Anisotropy in the Microwave Dielectric Properties of $SrTiO_3$ Films. *J. Appl. Phys.* **2005**, *98*, 024107. [CrossRef]
27. Biegalski, M.D.; Jia, Y.; Schlom, D.G.; Trolier-McKinstry, S.; Streiffer, S.K.; Sherman, V.; Uecker, R.; Reiche, P. Relaxor Ferroelectricity in Strained Epitaxial SrTiO3 Thin Films on $DyScO_3$ Substrates. *Appl. Phys. Lett.* **2006**, *88*, 192907. [CrossRef]
28. Haeni, J.H.; Irvin, P.; Chang, W.; Uecker, R.; Reiche, P.; Li, Y.L.; Choudhury, S.; Tian, W.; Hawley, M.E.; Craigo, B.; et al. Room-Temperature Ferroelectricity in Strained $SrTiO_3$. *Nature* **2004**, *430*, 758–761. [CrossRef]
29. Liang, L.; Liu, W.; Yan, X.; Zhang, Y.; Li, Z.; Yao, H.; Wang, Z.; Hu, X.; Li, Y.; Wu, G.; et al. Hybrid Amorphous Strontium Titanate and Terahertz Metasurface for Ultra-Sensitive Temperature Sensing. *Opt. Express* **2024**, *32*, 22578. [CrossRef]
30. Fareed, I.; Farooq, M.U.H.; Khan, M.D.; Ali, Z.; Butt, F.K. Band Gap Engineering of Strontium Titanate (SrTiO3) for Improved Photocatalytic Activity and Excellent Bio-Sensing Aptitude. *Mater. Sci. Semicond. Process.* **2024**, *177*, 108327. [CrossRef]
31. Zhang, D.; Li, C.; Han, S.; Diao, C.; Lou, G. Effect of BFO Layer Position on Energy Storage Properties of STO/BFO Thin Films. *J. Mater. Sci. Mater. Electron.* **2022**, *33*, 24078–24088. [CrossRef]
32. Caspi, S.; Baskin, M.; Shusterman, S.S.; Zhang, D.; Chen, A.; Cohen-Elias, D.; Sicron, N.; Katz, M.; Yalon, E.; Pryds, N.; et al. The Role of Interface Band Alignment in Epitaxial $SrTiO_3$ /GaAs Heterojunctions. *ACS Appl. Electron. Mater.* **2024**, *6*, 7235–7243. [CrossRef]
33. Khan, M.A.; Braic, L.; AlSalik, Y.; Idriss, H. Growth of Epitaxial Strontium Titanate Films on Germanium Substrates Using Pulsed Laser Deposition. *Appl. Surf. Sci.* **2021**, *542*, 148601. [CrossRef]
34. Tang, Y.; Zhu, Y.; Wu, B.; Wang, Y.; Yang, L.; Feng, Y.; Zou, M.; Geng, W.; Ma, X. Periodic Polarization Waves in a Strained, Highly Polar Ultrathin $SrTiO_3$. *Nano Lett.* **2021**, *21*, 6274–6281. [CrossRef] [PubMed]
35. Annam, R.S.; Danayat, S.; Nayal, A.; Tarannum, F.; Chrysler, M.; Ngai, J.; Jiang, J.; Schmidt, A.J.; Garg, J. Thickness Dependent Thermal Conductivity of Strontium Titanate Thin Films on Silicon Substrate. *J. Vac. Sci. Technol. A* **2024**, *42*, 022707. [CrossRef]
36. Okhay, O.; Vilarinho, P.M.; Tkach, A. Low-Temperature Dielectric Response of Strontium Titanate Thin Films Manipulated by Zn Doping. *Materials* **2022**, *15*, 859. [CrossRef]
37. Tumarkin, A.; Sapego, E.; Gagarin, A.; Bogdan, A.; Karamov, A.; Serenkov, I.; Sakharov, V. $SrTiO_3$ Thin Films on Dielectric Substrates for Microwave Applications. *Coatings* **2023**, *14*, 3. [CrossRef]
38. Kozyrev, A.; Ivanov, A.; Samoilova, T.; Soldatenkov, O.; Astafiev, K.; Sengupta, L.C. Nonlinear Response and Power Handling Capability of Ferroelectric $Ba_xSr_{1-x}TiO_3$ Film Capacitors and Tunable Microwave Devices. *J. Appl. Phys.* **2000**, *88*, 5334–5342. [CrossRef]
39. Soldatenkov, O.; Samoilova, T.; Ivanov, A.; Kozyrev, A.; Ginley, D.; Kaydanova, T. Nonlinear Properties of Thin Ferroelectric Film-Based Capacitors at Elevated Microwave Power. *Appl. Phys. Lett.* **2006**, *89*, 232901. [CrossRef]
40. Tumarkin, A.; Razumov, S.; Gagarin, A.; Altynnikov, A.; Mikhailov, A.; Platonov, R.; Kotelnikov, I.; Kozyrev, A.; Butler, J.E. Ferroelectric Varactor on Diamond for Elevated Power Microwave Applications. *IEEE Electron. Device Lett.* **2016**, *37*, 1. [CrossRef]
41. Wang, X.; Helmersson, U.; Madsen, L.D.; Ivanov, I.P.; Münger, P.; Rudner, S.; Hjörvarsson, B.; Sundgren, J.-E. Composition, Structure, and Dielectric Tunability of Epitaxial $SrTiO_3$ Thin Films Grown by Radio Frequency Magnetron Sputtering. *J. Vac. Sci. Technol. A Vac. Surf. Film.* **1999**, *17*, 564–570. [CrossRef]
42. Loginov, V.E.; Tumarkin, A.V.; Sysa, M.V.; Buslov, O.U.; Gaidukov, M.M.; Ivanov, A.I.; Kozyrev, A.B. The Influence of Synthesis Temperature on Structure Properties of $SrTiO_3$ Ferroelectric Films. *Integr. Ferroelectr.* **2001**, *39*, 375–381. [CrossRef]
43. Slifka, A.J.; Filla, B.J.; Phelps, J.M. Thermal Conductivity of Magnesium Oxide from Absolute, Steady-State Measurements. *J. Res. Natl. Inst. Stand. Technol.* **1998**, *103*, 357. [CrossRef]

44. Dörre, E.; Hübner, H. Alumina: Processing, Properties, and Applications. In *Materials Research and Engineering*; Springer: Berlin, Germany; New York, NY, USA, 1984; ISBN 978-0-387-13576-2.
45. Levinštejn, M.E.; Rumyantsev, S.L.; Shur, M. Properties of Advanced Semiconductor Materials GaN, AlN, InN, BN, SiC, SiGe. In *A Wiley-Interscience Publication*; Wiley: New York, NY, USA; Weinheim, Germany, 2001; ISBN 978-0-471-35827-5.
46. Clarke, R.C.; Palmour, J.W. SiC Microwave Power Technologies. *Proc. IEEE* **2002**, *90*, 987–992. [CrossRef]
47. Östling, M.; Koo, S.-M.; Zetterling, C.-M.; Khartsev, S.; Grishin, A. Ferroelectric Thin Films on Silicon Carbide for Next-Generation Nonvolatile Memory and Sensor Devices. *Thin Solid. Films* **2004**, *469–470*, 444–449. [CrossRef]
48. Lee, J.S.; Jo, Y.-D.; Koh, J.-H.; Ha, J.-G.; Koo, S.-M. Crystalline and Electrical Properties of BST/4H-SiC Capacitors. *J. Korean Phys. Soc.* **2010**, *57*, 1889–1892. [CrossRef]
49. Song, L.; Chen, Y.; Wang, G.; Yang, L.; Ge, J.; Dong, X.; Xiang, P.; Zhang, Y.; Tang, X. Fabrication and Dielectric Properties of $Ba_{0.63}Sr_{0.37}TiO_3$ Thin Films on SiC Substrates. *J. Am. Ceram. Soc.* **2014**, *97*, 3048–3051. [CrossRef]
50. Tumarkin, A.; Gagarin, A.; Odinets, A.; Zlygostov, M.; Sapego, E.; Kotelnikov, I. Structural and Microwave Characterization of $BaSrTiO_3$ Thin Films Deposited on Semi-Insulating Silicon Carbide. *Jpn. J. Appl. Phys.* **2018**, *57*, 11UE02. [CrossRef]
51. Koropov, A.V.; Ostapchuk, P.N.; Slezov, V.V. Diffusion-controlled growth of two-dimensional phases in ensembles. *Sov. Phys. Solid. State* **1991**, *33*, 1602–1607.
52. Kukushkin, S.A.; Osipov, A.V. Nucleation and Growth Kinetics of Nanofilms. In *Nucleation Theory and Applications*; Schmelzer, J.W.P., Ed.; Wiley: New York, NY, USA; Weinheim, Germany, 2005; pp. 215–255. ISBN 978-3-527-40469-8.
53. Tumarkin, A.V.; Zlygostov, M.V.; Serenkov, I.T.; Sakharov, V.I.; Afrosimov, V.V.; Odinets, A.A. Initial Stages of Growth of Barium Zirconate Titanate and Barium Stannate Titanate Films on Single-Crystal Sapphire and Silicon Carbide. *Phys. Solid. State* **2018**, *60*, 2091–2096. [CrossRef]
54. Afrosimov, V.V.; Il'in, R.N.; Sakharov, V.I.; Serenkov, I.T.; Yanovskii, D.V.; Karmanenko, S.F.; Semenov, A.A. Study of $YBa_2Cu_3O_{7-x}$ Films at Various Stages of Their Growth by Medium-Energy Ion Scattering. *Phys. Solid. State* **1999**, *41*, 527–533. [CrossRef]
55. Koebernik, G.; Haessler, W.; Pantou, R.; Weiss, F. Thickness Dependence on the Dielectric Properties of $BaTiO_3/SrTiO_3$-Multilayers. *Thin Solid. Films* **2004**, *449*, 80–85. [CrossRef]
56. Niu, F.; Wessels, B.W. Surface and Interfacial Structure of Epitaxial $SrTiO_3$ Thin Films on (001)Si Grown by Molecular Beam Epitaxy. *J. Cryst. Growth* **2007**, *300*, 509–518. [CrossRef]
57. Kozyrev, A.B.; Soldatenkov, O.I.; Samoilova, T.B.; Ivanov, A.V.; Mueller, C.H.; Rivkin, T.V.; Koepf, G.A. Response Time and Power Handling Capability of Tunable Microwave Devices Using Ferroelectric Films. *Integr. Ferroelectr.* **1998**, *22*, 329–340. [CrossRef]
58. Kozyrev, A.B.; Gaĭdukov, M.M.; Gagarin, A.G.; Altynnikov, A.G.; Razumov, S.V.; Tumarkin, A.V. Influence of Metal-Ferroelectric Contacts on the Space Charge Formation in Ferroelectric Thin Film Capacitors. *Tech. Phys. Lett.* **2009**, *35*, 585–588. [CrossRef]
59. Kozyrev, A.B.; Soldatenkov, O.I.; Ivanov, A.V. Switching Time of Planar Ferroelectric Capacitors Using Strontium Titanate and Barium Strontium Titanate Films. *Tech. Phys. Lett.* **1998**, *24*, 755–757. [CrossRef]